



## An integrated model for the post-solidification shape and grain morphology of fusion welds



Anton Kidess<sup>a,d,\*</sup>, Mingming Tong<sup>b</sup>, Gregory Duggan<sup>b</sup>, David J. Browne<sup>b</sup>, Saša Kenjereš<sup>a,d</sup>, Ian Richardson<sup>c</sup>, Chris R. Kleijn<sup>a,d</sup>

<sup>a</sup> Department of Chemical Engineering, Delft University of Technology, Julianalaan 136, 2628BL Delft, Netherlands

<sup>b</sup> School of Mechanical and Materials Engineering, University College Dublin, Belfield, Dublin 4, Ireland

<sup>c</sup> Department of Materials Science and Engineering, Delft University of Technology, Mekelweg 2, 2628CD Delft, Netherlands

<sup>d</sup> JM Burgers Centre for Fluid Mechanics, Mekelweg 2, 2628CD Delft, Netherlands

### ARTICLE INFO

#### Article history:

Received 17 October 2014

Received in revised form 5 January 2015

Accepted 31 January 2015

Available online 25 February 2015

#### Keywords:

Welding

Solidification

Simulation

Microstructure

Marangoni flow

### ABSTRACT

Through an integrated macroscale/mesoscale computational model, we investigate the developing shape and grain morphology during the melting and solidification of a weld. In addition to macroscale surface tension driven fluid flow and heat transfer, we predict the solidification progression using a mesoscale model accounting for realistic solidification kinetics, rather than quasi-equilibrium thermodynamics. The tight coupling between the macroscale and the mesoscale distinguishes our results from previously published studies.

The inclusion of Marangoni driven fluid flow and heat transfer, both during heating and cooling, was found to be crucial for accurately predicting both weld pool shape and grain morphology. However, if only the shape of the weld pool is of interest, a thermodynamic quasi-equilibrium solidification model, neglecting solidification kinetics, was found to suffice when including fluid flow and heat transfer.

We demonstrate that the addition of a sufficient concentration of approximately 1  $\mu\text{m}$  diameter TiN grain refining particles effectively triggers a favorable transition from columnar dendritic to equiaxed grains, as it allows for the latter to heterogeneously nucleate in the undercooled melt ahead of the columnar dendritic front. This transition from columnar to equiaxed growth is achievable for widely differing weld conditions, and its precise nature is relatively insensitive to the concentration of particles and to inaccurately known model parameters.

© 2015 Elsevier Ltd. All rights reserved.

### 1. Introduction

Welding is a ubiquitous industrial process of great economic and technological importance [1]. Welding processes involve complex physical phenomena spanning multiple length and time scales [2]. In particular, fusion welding processes involve phase changes, heat transfer by conduction, convection and radiation, as well as surprisingly strong fluid flow driven by Marangoni effects (gradients in surface tension), all of which are tightly coupled to one another.

Key mechanical properties of alloy welds are related both to (i) their shape and to (ii) their grain structure, and thus it is highly desirable to exert as much control as possible on both during weld formation. Whereas the shape is mainly determined by macroscopic phenomena such as heat transfer and Marangoni driven fluid flow during the melting phase, and can be largely influenced by

modifying the fluid flow through the addition of surface active species [3,4], the grain structure is mainly determined by mesoscopic (grain scale) crystallization phenomena during solidification of the melt, and can be controlled by the addition of non-melting grain refining particles [5–9].

Typically, the grain morphology of a post-solidification weld consists of columnar dendrites, characterized by elongated, tree-like columns of solid which have grown into the melt. Equiaxed solidification, where solidification nucleation occurs within the melt away from the columnar front, is not common, as the thermal gradient ahead of the solidification front is too large to allow for the necessary undercooling for equiaxed growth to occur [6,10]. However, the transition of the common columnar solidification mode to equiaxed solidification is of practical interest. Equiaxed material is less prone to the unwanted hot-cracking (tears appearing in the fusion zone near the end of the solidification process [11]) and also impedes the undesired segregation of alloying elements to the central plane of the weld [5,7,12].

\* Corresponding author at: Department of Chemical Engineering, Delft University of Technology, Julianalaan 136, 2628BL Delft, Netherlands.

E-mail address: [A.Kidess@tudelft.nl](mailto:A.Kidess@tudelft.nl) (A. Kidess).

## Nomenclature

|                  |  |
|------------------|--|
| $C$              | dendrite kinetics coefficient                            |
| $C_0$            | alloy composition  |
| $C_p$            | heat capacity  |
| $\frac{D}{D_f}$  | material derivative                                      |
| $d_{min}$        | minimum diameter of nucleating particles                 |
| $D_l$            | diffusion coefficient of solute in the liquid            |
| $F(d)$           | cumulative distribution function for equiaxed nucleation |
| $\bar{F}_{damp}$ | momentum sink term due to solidification                 |
| $f_s$            | volume fraction of solid in mush                         |
| $g$              | volume fraction of solid                                 |
| $h$              | convective heat transfer coefficient                     |
| $k_q$            | gaussian distribution coefficient                        |
| $L$              | latent heat  |
| $m$              | slope of the liquidus line                               |
| $N$              | count of nucleated particles                             |
| $P$              | laser power  |
| $p$              | pressure   |
| $\dot{q}$        | heat flux  |
| $R$              | volume averaged dendrite envelop radius                  |
| $r_q$            | $1/e^2$ radius for Gaussian distribution                 |
| $S_{latent}$     | latent heat source term                                  |
| $\Delta S_v$     | fusion entropy   |
| $T$              | temperature  |
| $\Delta T_c$     | local undercooling                                       |
| $T_\infty$       | ambient temperature                                      |
| $T_s, T_l$       | solidus and liquidus temperature                         |
| $\vec{U}$        | fluid velocity   |

|            |  |
|------------|--|
| $v$        | dendrite tip velocity                        |
| $V_{equi}$ | volume of equiaxed dendrites                 |
| $V_{ex}$   | volume of existing equiaxed dendrites        |
| $V_{new}$  | volume of newly nucleated equiaxed dendrites |

### Greek symbols

|                |   |
|----------------|---|
| $\alpha$       | partition coefficient   |
| $\epsilon$     | emmissivity   |
| $\eta$         | laser absorptivity  |
| $\Gamma$       | Gibbs Thomson coefficient   |
| $\gamma$       | surface tension   |
| $\gamma_{sl}$  | solid-liquid interfacial tension  |
| $\lambda$      | thermal conductivity  |
| $\mu$          | dynamic viscosity   |
| $\mu_{1/2}$    | median inoculant diameter   |
| $\phi_{col}$   | volume fraction of columnar dendrites   |
| $\phi_{equi}$  | volume fraction of equiaxed dendrites after taking into account grain impingement |
| $\phi_s$       | volume fraction of mush   |
| $\rho$         | density   |
| $\rho_{seeds}$ | inoculant particle number density   |
| $\sigma_b$     | Stefan Boltzman constant  |
| $\sigma_d$     | standard deviation for the log-normal distribution of inoculant diameters         |

### Subscripts

|     |                      |
|-----|----------------------|
| $n$ | normal direction     |
| $t$ | tangential direction |

Since quantitative experimental research of macroscopic shape evolution and mesoscopic structure evolution in welds is tremendously difficult to conduct [13], there is a need for efficient, realistic numerical models that can predict both [14].

The majority of previously published numerical studies (e.g. [4,15–18]) on macroscopic phenomena during welding have focused on the evolution of the weld pool shape and temperature up to the end of the melting stage, and thus neglect further changes in the weld pool shape during re-solidification after the heat source has been removed. However, it has been shown that the shape of the weld pool can still change significantly during the subsequent re-solidification [19,20]. A proper study of macroscopic weld formation should therefore include the solidification stage.

Other previous studies have focused on predicting the post-solidification mesoscopic grain structure of the weld, which is entirely determined during the solidification stage. In these studies the microstructure was either studied by a posteriori analysis, neglecting undercooling of the melt and the possibility of heterogeneous nucleation sites (e.g. [18]), or the solidification progression was modeled using mesoscopic models, while neglecting the influence of macroscopic phenomena such as fluid flow in the molten metal on the weld pool shape [5,21–25].

However, the macroscale and the mesoscale cannot be separated, as macroscale phenomena such as fluid flow and heat transfer determine the evolution of solidification on the mesoscale as well. Therefore, a proper prediction of weld properties requires a combination of both types of modeling. In this paper we present such an integrated macroscale/mesoscale model and we show that it can be used to simultaneously predict the macroscopic shape and the mesoscopic grain structure of a solidified conduction-mode laser weld. On the macroscale, we compute the heat transfer and (thermocapillary driven) fluid flow in the weld. On the mesoscale, the solidification evolution is determined from actual interface

kinetics, rather than interface equilibrium assumptions. With this integrated model, we investigate the role of fluid flow during solidification, and the possible alteration of the solidification mesostructure in a steel alloy laser weld using grain refining particles.

## 2. Mathematical formulation

### 2.1. Governing equations

A schematic of a typical stationary weld is shown in Fig. 1, where a non-moving slab of metal is targeted by a fixed high power laser. The laser irradiation will be absorbed by the target mate-

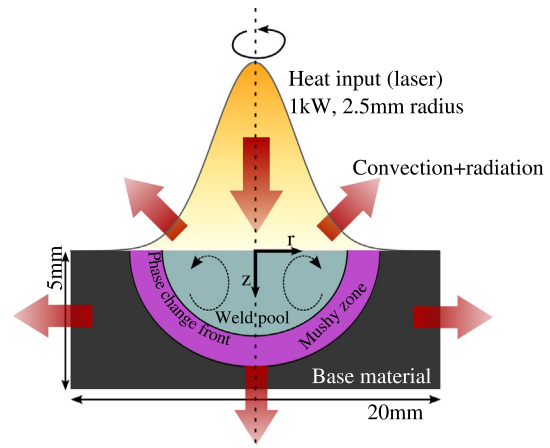


Fig. 1. Schematic representation of the studied laser welding. The domain is assumed to be axisymmetric.

Download English Version:

<https://daneshyari.com/en/article/7056701>

Download Persian Version:

<https://daneshyari.com/article/7056701>

[Daneshyari.com](https://daneshyari.com)